JOURNAL OF Applied Polymer SCIENCE

In situ thermal polymerization of an ionic liquid monomer for quasi-solid-state dye-sensitized solar cells

Pingyuan Song, Minda Gao, Ying Su, Jie Zhao, Guifu Zou

College of Physics, Optoelectronics and Energy & Collaborative Innovation Center of Suzhou Nano Science and Technology, Soochow University, Suzhou 215006, People's Republic of China

Correspondence to: J. Zhao (E-mail: jzhao@suda.edu.cn) and G. F. Zou (E-mail: zouguifu@suda.edu.cn)

ABSTRACT: *In situ* thermal polymerization of a model ionic liquid monomer and ionic liquids mixture to form gel electrolytes is developed for quasi-solid-state dye-sensitized solar cells (Q-DSSCs). The chemical structures and thermal property of the monomers and polymer are investigated in detail. The effect of iodine concentration on the conductivity and triiodide diffusion of the gel electrolytes is also investigated in detail. The conductivity and triiodide diffusion of the gel electrolytes increase with the increasing I_2 concentration, while excessive I_2 contents will decrease the electrical performances. Based on the *in situ* thermal polymeric gel electrolytes for Q-DSSCs, highest power conversion efficiency of 5.01% has been obtained. The superior long-term stability of fabricated DSSCs indicates that the cells based on *in situ* thermal polymeric gel electrolytes can overcome the drawbacks of the volatile liquid electrolyte. These results offer us a feasible method to explore new gel electrolytes for high-performance Q-DSSCs. © 2015 Wiley Periodicals, Inc. J. Appl. Polym. Sci. **2015**, *132*, 42802.

KEYWORDS: conducting polymers; electrochemistry; ionic liquids; photochemistry

Received 11 June 2015; accepted 3 August 2015

DOI: 10.1002/app.42802

INTRODUCTION

Due to their low production cost, easy-handing fabrication, and high power conversion efficiencies, dye-sensitized solar cells (DSSCs) have attracted a great deal of interest.[1–16] Recently, impressive efficiencies over 13% have been successfully achieved by employing cobalt(II/III)-based liquid electrolytes in conjunction with donor–π-bridge–acceptor zinc porphyrin dyes.[3,4] Unfortunately, volatilization and leakage of organic solvent increase the sealing difficulty and restrain the long-term stability of DSSCs under outdoor working condition.[5] To overcome the resultant problems, considerable reports have been proposed to develop stable solid and quasi-solid-state electrolytes for DSSCs.[2,5] Although *p*-type semiconductors and hole conductors can solve some of these problems, the photoelectrical conversion efficiencies of these cells are still low and the stability is not satisfactory for practical use because of low hole-conductivity, formation of crystals, and poor semiconductor–electrolyte interface interaction.[8,11] Recently, due to their unique hybrid matrix and favorable properties, such as thermal stability, high ionic conductivity, good contacting, and filling properties,[6] quasi-solid-state dye-sensitized solar cells (Q-DSSCs) based on nanocomposite gel and polymer gel electrolytes have attracted growing attention.[4,5,8,15,16] Based on these polymer gel electrolytes, comparable efficiencies to the cells with liquid electrolytes have been obtained due to their favorable properties such as high ionic conductivity, good contacting with the nanocrystalline TiO_2 electrode, and counter electrode.[5,9]

In virtue of their negligible vapor pressure, high chemical and thermal stability, nonflammability, high ionic conductivity, and wide electrochemical window,[17,18] ionic liquids (ILs) have been widely used as an important source for iodide-based redox couple electrolytes in DSSCs.[5,11] Unfortunately, there are still a potential problem of ionic liquid electrolytes, which require rigorous and perfect sealing to prevent leakage for their wide-spread applications.

Recently, incorporating ionic liquids into matrix materials have been investigated to improve the leakage and evaporation durability for Q-DSSCs.[8,11] Various materials, such as ethylene oxide copolymer,[9] acrylonitrile copolymer,[19] methylmethacrylate copolymer,[20] vinylidenefluoride copolymer,[3] low-molecular-weight organic gelators,[21] nematic liquid crystals,[22] and inorganic particles[3,5,7] have been used to fabricate Q-DSSCs.

In order to obtain high efficiencies and high-temperature stability for quasi-solid-state DSSCs, an ideal gel electrolyte would

Additional Supporting Information may be found in the online version of this article.

contain nonvolatile organic plasticizers and solvents, high ionic conductivity, high thermal stability, and good filling properties. In general, quasi-solid-state electrolytes have difficulty in permeating into the pores of TiO_2 photoelectrodes because of high polymer molecular weight and gel viscosity.[23] Therefore, *in situ* polymerization of monomers to form a cross-linked polymer network would overcome the problem, achieving a satisfactory filling of electrolytes and good contacts.[23–28] However, because of very low ionic conductivity, these polymer hosts just acted as stiffeners for the solvent, just creating a three-dimensional network to provide the ions migration,[8] and their solubility must be mostly in virtue of organic plasticizers. For outdoor use, however, the presence of volatile plasticizers in the Q-DSSCs still holds the potential problems such as high-temperature flammability and instability.[21]

In this study, we report an *in situ* thermal polymerization of a model ionic liquid monomer, [BVIm] [TFSI] in an ILs mixture. After polymerization, a certain I_2 is introduced by sublimation in a closed container (volume: 50 mL) at 40°C for 24 h. Such organic solvent-free high-performance quasi-solid-state electrolytes for DSSCs could overcome the drawbacks of cells based on liquid and polymer electrolytes containing conventional volatile organic solvent plasticizers. In addition, the polymer host from the monomer [BVIm] [TFSI] shows a higher conductivity compared with conventional polymers, which does not clearly decrease the conductivity of the resultant gel electrolytes. Furthermore, the conductivity and device performance were optimized by tuning the amount of I_2 introduced to the gel electrolytes.

EXPERIMENTAL

Materials

1-Iodopropane, 1-bromoethane, 1-bromobutane, 1-methylimidazole, 1-vinylimidazole, 4-*tert*-butylpyridine (TBP), 2,2′-azobis(isobutyronitrile) (AIBN), lithium iodide, and lithium bis(trifluoromethanesulphonyl)imide (LiTFSI) were purchased from Alfa Aesar and used as received. $TiCl_4$ and H_2PtCl_6 were purchased from Aldrich (China). cis-RuLL′(SCN)$_2$ (L = 4,4′-dicarboxylicacid-2,2′-bipyridine, L′ = 4,4′-dinonyl-2,2′-bipyridine), abbreviated as Z907, was provided by Solaronix SA (Switzerland) and used without further purification. Fluorine-doped tin oxide overlayer (FTO) glass electrodes (15 Ω/cm^2), 20-nm-sized mesoporous and light-scattering anatase TiO_2 colloidal (diameter: 200 nm) slurries were purchased from HepatChroma SolarTech Co., Ltd (Dalian, China) and used without further treatment.

Characterization and Photovoltaic Measurements

^{1}HNMR spectra were carried out on a Varian 400 MHz spectrometer. Fourier transform infrared (FTIR) spectra were recorded on a ProStar LC240 FTIR spectrometer in the range of 4000–400 cm^{-1}. The Labram HR800 microRaman spectrometer equipped with a 514-nm argon laser (25 mW) was used in recording the Raman spectra. ^{1}HNMR spectra were conducted on a UNITY INOVA 400 spectrometer. To better evaluate the polymer based on *in situ* thermal polymerization, the molecular weight (Mn = 22,300) and degree (PDI = 1.95) of polymerization were measured by gel permeation chromatography (GPC) using a Waters Styragel HR 5 column and *N*,*N*-dimethylformamide containing 0.02% lithium bromide as eluent. Surface morphologies were investigated by SEM (Hitachi SU8010) at an accelerating voltage of 5 kV. The conductivity of gel electrolytes was characterized in an ordinary cell composed of Teflon tube and two identical stainless steel electrodes (diameter of 1 cm) on a CHI660c electrochemical workstation at room temperature, using the AC impedance method over the frequency range 0.1–10^5 Hz. The conductivity was obtained using the following equation:[40]

$$\sigma = \frac{l}{RS} \tag{1}$$

where σ is the conductivity in S cm^{-1}, R is the ohmic resistance of the electrolyte, l is the distance between two electrodes, and S is the area of the electrodes.

The diffusion coefficients (D_{app}) of I_3^- can be calculated from the cathodic steady-state currents (I_{ss}) using the following equation:[5]

$$I_{ss} = 4nFD_{app}C\gamma \tag{2}$$

where n is the number of electrons per molecule, F is the Faraday constant, γ is the radius of the ultramicroelectrode, and C is the bulk concentration of the electroactive species.

The photocurrent density–voltage (J–V) curves of the assembled DSSCs shielded by an aluminum-foil mask with an aperture area of 0.1 cm^2 were measured with a digital source meter (Keithley, model 2612) under AM 1.5 simulated solar illumination at 100 mW cm^{-2}. Incident photon-to-current conversion efficiency (IPCE) plotted as a function of excitation wavelength was recorded on a Keithley 2400 Source Meter under the irradiation of a 300 W xenon lamp with a monochromator (Oriel CornerstoneTM 260 1/4). The photoelectrochemical parameters, such as open-circuit voltage (V_{oc}), short-circuit photocurrent density (J_{sc}), PCE, and IPCE were obtained according to the previous reports.[9,30]

Synthesis of Room Temperature ILs and Monomers

Room temperature ionic liquids—1-propyl-3-methylimidazolium iodide (PMII) and 1-ethyl-3-methylimidazolium bis((trifluoromethyl)sulfonyl)imide (EMITFSI)—were synthesized as a reference in the literature.[29] An IL monomer, 1-butyl-3-vinylimidazolium bromide ([BVIm] [Br]) (primrose yellow), was synthesized by the reaction of 1-bromobutane with 1-vinylimidazole for 3 days at room temperature.[37] ^{1}HNMR: (400 MHz, $CDCl_3$): 11.04 (s, 1H), 7.80 (s, 1H), 7.53 (s, 1H), 7.50 (q, 1H), 6.00 (dd, 1H), 5.40 (dd, 1H), 4.42 (t, 3H), 1.94(m, 2H), 1.40(m, 2H), 0.96 (*t*, 3H). (Yield: 74%). Microanalysis Calcd.: C, 46.77%; H, 6.54%; N, 12.12%. Found: C, 46.27%; H, 6.70%; N, 12.32%. IR (ν_{max}, liquid film, cm^{-1}): 3527 [ν(imidazolium)$_{arom}$], 2941, 2863 [ν(CH)$_{aliph}$], 1652 [ν[C═C], 1557[ν(CH)$_{arom}$], 1170[ν(C—C, C—N)$_{arom}$]. Anion exchange[38] of [BVIm] [Br] with LiTFSI in aqueous solution yielded 1-butyl-3-vinylimidazolium bis(trifluoromethanesulph-onyl)imide ([BVIm] [TFSI]) (colorless). ^{1}HNMR: (400 MHz, $CDCl_3$): 9.06 (s, 1H), 7.60 (*t*, 1H), 7.41 (*t*, 1H), 7.13 (q, 1H), 5.78 (m, 1H), 5.44 (m, 1H), 4.24 (*t*, 3H), 1.88(m, 2H), 1.38(m, 2H), 0.97 (*t*, 3H). (Yield: 84%). Microanalysis Calcd.: C, 30.63%; H, 3.50%; N, 9.74%; S, 14.87%. Found: C, 30.28%; H, 3.42%; N, 9.80%; S, 15.03%. IR (ν_{max}, liquid film, cm^{-1}): 3518 [ν(imidazolium)$_{arom}$], 3150 [ν(CH)$_{arom}$], 2967,

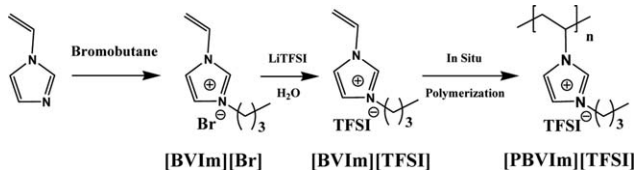

Scheme 1. Synthetic procedure for the preparation of model ionic liquids monomers.

2879 [$\nu(CH)_{aliph}$], 1643 [ν[C═C], 1558 [$\nu(CH)_{arom}$], 1354 [$\nu(SO_2)$], 1203 [$\nu(SO_2)$], 1046 [ν(SNS)].

Preparation of Ionic Liquid Monomer/ILs Mixture

[BVIm] [TFSI] (25 wt %) was dissolved into liquid mixtures containing 0.1*M* LiI, 0.5*M* TBP, AIBN (2.5 wt % of [BVIm] [TFSI]), and a mixture of PMII and EMITFSI (volume ratio of 13 : 7). This ILs mixture is denoted as BASIC.

Fabrication of Q-DSSCs[39]

A doctor-bladed double layer of TiO_2 particles was used as the photoanode. A 10-μm-thick film of 20-nm-sized TiO_2 particles was first deposited onto the FTO glass electrode and further coated by a 4-μm-thick second layer of 200-nm diameter, light-scattering particles. The resulting TiO_2 films were annealed at 500°C for 30 min. After cooling to 80°C, the obtained TiO_2 electrode was immersed in 0.3m*M* solution of Z907 in acetonitrile and *tert*-butyl alcohol at room temperature for 12 h. To prepare the Pt counter electrode, two drops of 5m*M* H_2PtCl_6 in ethanol was placed onto the cleaned FTO glass substrate, followed by drying and annealing at 400°C for 15 min. The electrodes were separated by a 25-μm-thick hot melting ring (Surlyn, Dupont) and sealed up by heating. The internal space was filled with the BASIC using a vacuum back filling system for 10 h at 50°C, then was *in situ* polymerized at 80°C under a nitrogen atmosphere for 8 h. After the completion of the polymerization, a certain I_2 was introduced by sublimation in a closed container (volume: 50 mL) at 40°C for 24 h. The amount of I_2 introduced into gel electrolytes could be controlled by sublimation time and added initial amount of I_2. The mass ratio of I_2/I^- was from 0 to 2. The electrolyte-injecting hole on the counter electrode glass substrate was sealed with a hot melting sheet and a thin glass cover by heating.

RESULTS AND DISCUSSION

Scheme 1 showed the general synthetic process of the polymer [PBVIm] [TFSI] to combine with the BASIC to form gel electrolytes for Q-DSSCs. The purity and chemical structures of monomers are confirmed by ^1H nuclear magnetic resonance (NMR) (Supporting Information, Figures S1 and S2).

The chemical structures of monomers and polymer were further confirmed by FTIR spectra in Figure 1. The polymer [PBVIm] [TFSI] also represents good thermal stability over 350°C (Supporting Information, Figure S3). In all FTIR spectra, the characteristic peaks of imidazole cation in the range of 3200–3600 cm^{-1} were observed. As shown in Figure 1(a), the absorption peaks at 1170, 1160, and 1125 cm^{-1} were assigned to the stretching and asymmetric stretching vibrations of C—N of imidazole rings.[37] Compared with Figure 1(a), new bands corresponding to TFSI anion were observed at 1354, 1203, and 1046 cm^{-1} in Figure 1(b) indicating the anion exchange of the monomer [BVIm] [TFSI]. *In situ* thermal polymerization of [BVIm] [TFSI] in a TiO_2 photoanode is carried out by heating the [BVIm] [TFSI] at 80°C for 8 h to obtain resulting polymer [PBVIm] [TFSI] for FTIR testing. Thus, the absorption band [Figure 1(c)] disappears after successful polymerization at around 1643 cm^{-1} [Figure 1(b)], which is ascribed to the C═C stretching band of monomer [BVIm] [TFSI].

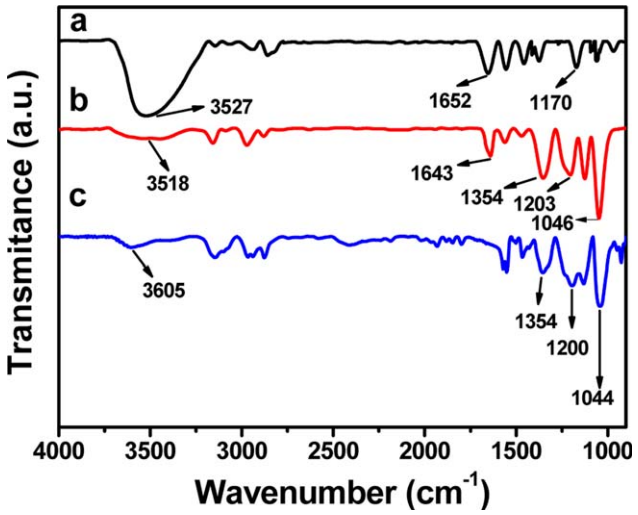

Figure 1. FTIR spectra of (a) [BVIm] [Br]; (b) [BVIm] [TFSI]; and (c) [PBVIm] [TFSI]. [Color figure can be viewed in the online issue, which is available at wileyonlinelibrary.com.]

Because iodine is a potent free-radical inhibitor, after *in situ* polymerization, a series of electrolytes were prepared by adding different iodine contents and stirring at 40°C for 12 h. As shown in Figure 2 and Table I, the influence of these electrolytes on conductivity and triiodide diffusion was investigated, which could be referential significance for preparation and optimization for the following Q-DSSCs. The curves are also present in Figures S4 and S5 in Supporting Information. An increased

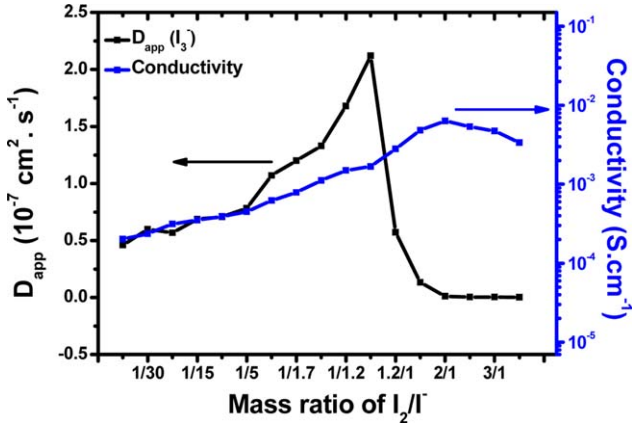

Figure 2. The influence of I_2 concentration on the conductivity and triiodide diffusion coefficients of poly(ionic liquids)-based gel electrolytes. [Color figure can be viewed in the online issue, which is available at wileyonlinelibrary.com.]

Table I. Electrical Parameters of Q-DSSCs Containing Different I_2 Concentrations

Mass ratio of I_2/I^{-a}	σ (10^{-4} S cm^{-1})	D_{app} (I_3^-) ($10^{-7}cm^2$ s^{-1})	J_{sc} (mA cm^{-2})	V_{oc} (V)	FF	η (%)
0	1.46	0	7.16	0.682	0.687	3.35
1/40	2.02	4.60	8.87	0.677	0.684	4.11
1/20	3.14	5.67	10.06	0.662	0.721	4.80
1/10	3.92	7.07	10.50	0.651	0.718	4.91
1/1	16.8	13.3	11.32	0.621	0.710	5.01
2/1	51.3	9.41	8.35	0.601	0.678	3.40
3/1	47.1	2.57	6.13	0.570	0.610	2.13
4/1	33.8	1.19	4.97	0.547	0.630	1.72

[a] Thermal polymerization of 0.1*M* LiI, 0.5*M* TBP, [BVIm] [TFSI] (25 wt %), and AIBN (2.5 wt % of [BVIm] [TFSI]) in a mixture of PMII/EMITFSI (13 : 7, V/V), and adding different I_2 to form different gel electrolytes.

iodine introduced into the electrolytes will result in a polyiodide system.[10] Owing to a mechanism of electrical conduction in polyiodine chains via a Grotthus mechanism, the conductivity and mass transport of triiodide depends on the concentration of iodine. The conductivity increased from 1.46 to 16.8 $\times$ 10^{-4} S cm^{-1} with an increase of the mass ratio of I_2/I^- from 0 to 2/1 because of the formation of polyiodide chains by PMII and LiI combining with I_2. However, higher concentration of I_2 will reduce the conductivity, which probably results from the increased block influence of polyiodide carrier transferring.[10] Similarly, with an increase of the mass ratio of I_2/I^- from 0 to 1/1, the triiodide diffusion coefficient increase from 0 to 13.3 $\times$ 10^{-8} cm^2 s^{-1}. With much more increasing I_2, owing to the more formation of I_5^-, I_7^-, ..., I_{2n+1}^-, the concentration of I_3^- greatly decreased, which lead to an obvious decrease of mass transport and diffusion coefficient of I_3^-.

Raman spectra in the range of 50–350 cm^{-1} of the previous gel electrolytes was showed in Figure 3 in order to get insights into the general speciation of iodine-containing entities. The absorption bands at 114 cm^{-1} was the symmetric stretching vibration of I_3^- ions,[25,31] and the weaker band at 142–160 cm^{-1} was assigned to characterize the asymmetric stretching mode of I_3^- ions.[32] However, higher concentrations of iodine introduced could produce more amounts of polyiodide, which weaken these spectral features. In Figure 3, the gel electrolyte without iodine displayed no peaks, indicative of triiodide ions absent in the electrolyte [Figure 3(a)]. With an iodine concentration increase [mass ratio of I_2/I^- was 1/10, Figure 3(b)], the feature peaks at 114 and 151 cm^{-1} of triiodide ions were present. The intensity at 114 cm^{-1} was about 1.40 times stronger than the shoulder at 151 cm^{-1}. However, the intensity ratio was 1.57 times with an iodine concentration [mass ratio of I_2/I^- was 1/1, Figure 3(c)], indicating the form of a higher triiodide ions. Obviously, much higher iodine concentration would lead to the formation of more complicated polyiodide system. Particularly, it could greatly decrease the triiodide ions concentration, resulting in weaker Raman spectral features [Figure 3(d,e)].

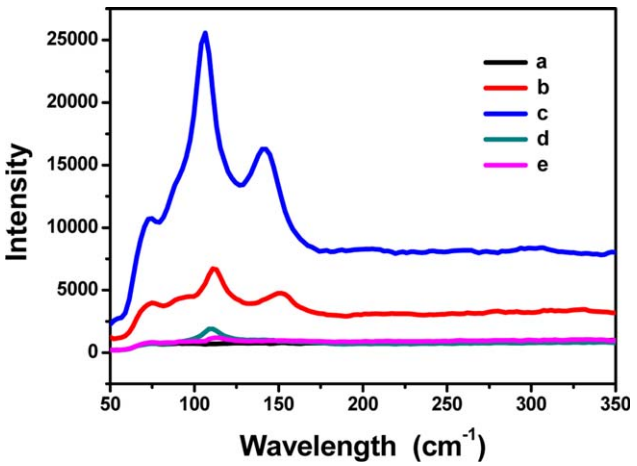

Figure 3. Raman spectra of poly(ionic liquids)-based gel electrolytes containing different I_2 concentrations. Mass ratio of I_2/I^-: (a) 0; (b) 1/10; (c) 1/1; (d) 2/1; and (e) 3/1. [Color figure can be viewed in the online issue, which is available at wileyonlinelibrary.com.]

Figure 4 shows the typical cross-section SEM image of a dyed photoanode coated with the gel electrolyte by an *in situ* thermal polymerization of the BASIC. It could be found that *in situ* thermal polymerization of monomer [BVIm] [TFSI] in BASIC could get smooth surface morphology on the dyed photoanode without obvious voids or particles, indicating good infiltration and filling of gel electrolytes based on this method.

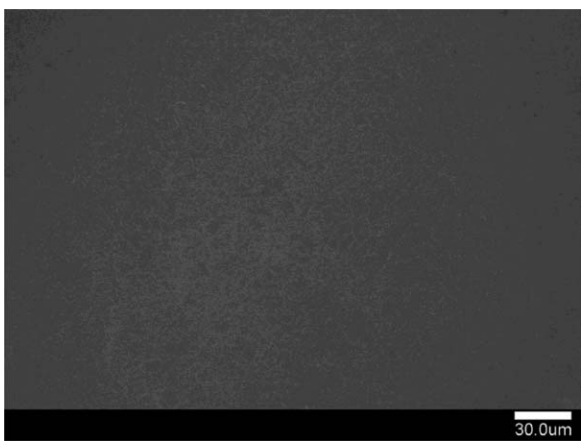

Figure 4. Typical cross-section SEM image of a dyed photoanode coated with the gel electrolyte by *in situ* thermal polymerization of the BASIC.

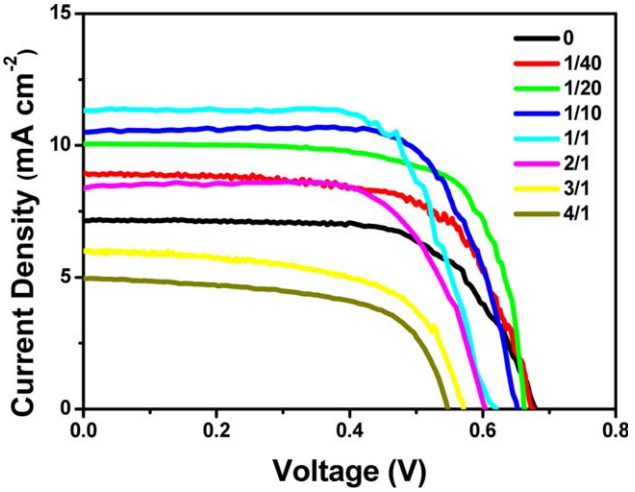

Figure 5. The *J–V* curves of DSSCs containing different I_2 concentrations under simulated AM 1.5 solar cell spectrum irradiation at 100 mW cm^{-2}. Cells are tested using an aluminum-foil mask with an aperture area of 0.1 cm^2. [Color figure can be viewed in the online issue, which is available at wileyonlinelibrary.com.]

Figure 5 shows the *J–V* curves of the fabricated DSSCs containing various iodine concentrations with the previous *in situ* thermal polymerization of the BASIC under simulated AM 1.5 solar spectrum illumination at 100 mW cm^{-2}. The photovoltaic parameters including V_{oc}, J_{sc}, FF, and PCE of DSSCs were summarized in Table I. The best result was obtained for the device fabricated with a proper amount of iodine (mass ratio of I_2/I^- was 1/1). The device showed J_{sc} of 11.32 mA cm^{-2}, V_{oc} of 0.621, FF of 0.710, and yielded a PCE of 5.01%. It could be found that adding the proper amounts of iodine had clearly increased the efficiency to a maximum value and then decreased under further additions. Interestingly, the increase or decrease of efficiency was not linear with the changes of the ionic conductivity and triiodide diffusion coefficients. This inconsistency also had been previously observed by other researchers. Kang's group reported the efficiency increases almost linearly with an increase in the log of the ionic conductivity.[33] However, Nogueira and coworkers found that the increase and diffusion of iodide species was important to the enhancement of photocurrent generation but not the ionic conductivity.[34] Lin's group also found that the diffusion of triiodide ions was a key effect on the efficiency of DSSCs.[4] In this case, it was supposed that increasing the contents of iodine could increase the concentration of polyiodides in the porous dye-sensitized TiO_2 matrix, which would greatly enhance the recombination of conductive band electrons with polyiodides such as I_5^-, I_7^-, and so on,[35,36] and obviously increased the dark current. In addition, the concentration loss of the additive TBP during the thermal polymerization process should be responsible for the recombination of conductive band electrons with polyiodides, which would also

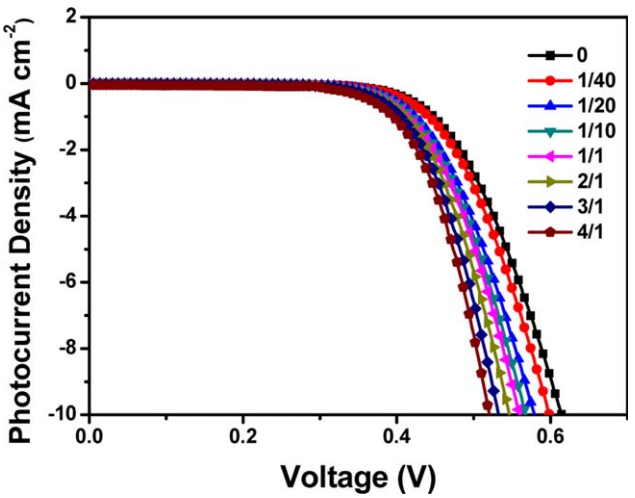

Figure 6. Dark current–voltage characteristics of Q-DSSCs fabricated with different I_2 concentrations. [Color figure can be viewed in the online issue, which is available at wileyonlinelibrary.com.]

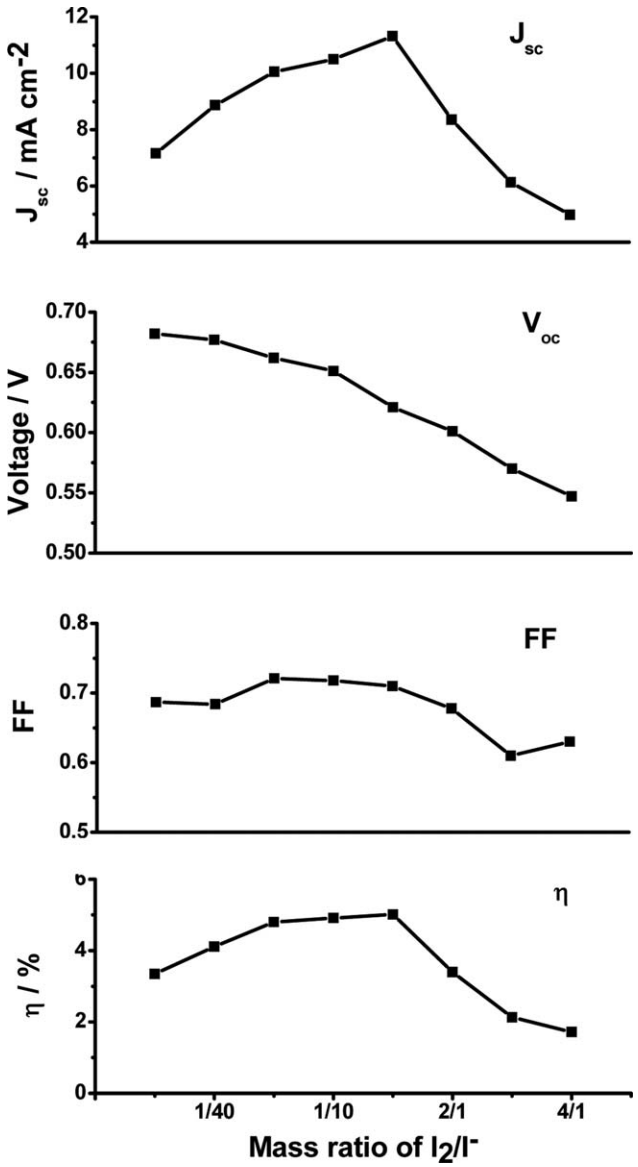

Figure 7. Effect of I_2 variation on the photovoltaic characteristics of DSSCs employing poly(ionic liquids)-based gel electrolytes.

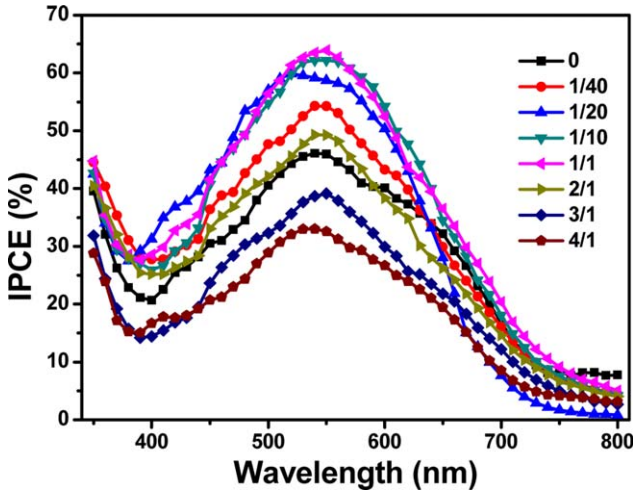

Figure 8. The IPCE *vs* wavelength profiles for Q-DSSCs based on *in situ* polymerization gel electrolytes containing different I_2 concentrations. [Color figure can be viewed in the online issue, which is available at wileyonlinelibrary.com.]

lead to the increase of the dark current and the decrease of J_{sc}, especially at high I_2 concentrations.

The V_{oc} variation of DSSCs had a great relationship with the dark current, which originated mainly from the reduction of I_3^- by conduction band electrons from TiO_2, according to the following equation:[30]

$$V_{oc} = \frac{kT}{e} In\left(\frac{I_{inj}}{n_{cb} k_{et} [I_3^-]}\right) \quad (3)$$

Where I_{inj} is the flux of charge resulting from sensitized injection related to the electron back transfer rate, n_{cb} is the concentration of electrons at the TiO_2 surface, and k_{et} is the rate constants for I_3^- reduction. As shown in Figure 6, the onset of the potential shifted from 0.36 to 0.29 V with an increase of I_2 concentrations (mass ratio of I_2/I^-: 0–4/1), indicating a higher I_3^- reduction rate (k_{et}), leading to a decrease of V_{oc}, according to the previous equation.

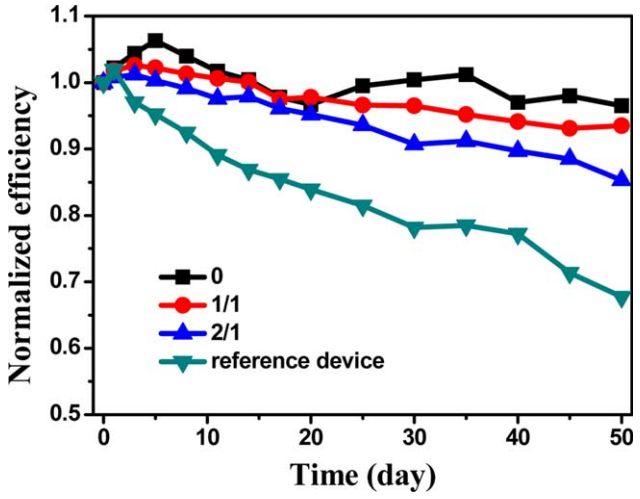

Figure 9. Changes in the normalized photoconversion efficiency of DSSCs based on different I_2 concentrations. Mass ratio of I_2/I^-: (a) 0; (b) 1/1; and (c) 2/1. A typical organic liquid electrolyte for the reference device contains 0.6*M* DMPII, 0.1*M* LiI, 0.5*M* TBP, 0.1*M* I_2 in MPN.[40] [Color figure can be viewed in the online issue, which is available at wileyonlinelibrary.com.]

As can be seen from Figure 7, obvious changing trends of J_{sc} and V_{oc} were observed as previously described. However, it seemed that higher I_2 concentrations would clearly decrease the FF of the devices, which was mainly limited by the recombination of conductive band electrons with polyiodides. Therefore, an appropriate I_2 concentration (mass ratio of I_2/I^-: 1/1) for the highest PCE of 5% was obtained.

Figure 8 represents the IPCE of devices based on poly(ionic liquids)-based gel electrolytes containing different I_2 concentrations were consistent with the previous efficiencies. The maximum IPCE values at about 540 nm were 46%, 54%, 60%, 62%, 64%, 49%, 40%, and 33%, respectively. Corresponding to the UV absorbing characteristic of Z907 dye, the relatively broad features appeared covering the visible spectrum range from 450 to 650 nm, indicating high light harvesting and device performance.

As shown in Figure 9, the long-term stability of the three representative Q-DSSCs was investigated with successive one sun light soaking during the accelerated aging test at 60°C. For comparison, referenced device with an organic liquid-state electrolyte was also tested at the same condition. The efficiencies of the devices were measured in every 3 or 5 days, and normalized to the values tested on the first day. During the first 5 days, the efficiencies of all the poly(ionic liquids)-based cells increased due to the increased regeneration rate of dye. However, the efficiencies decreased gradually. It should be noted that the DSSCs fabricated with low I_2 concentrations still maintained over 94% of their initial efficiency after 50 days, whereas the high I_2 concentration might increase the dark current, weakening the performance durability of a DSSC. However, compared with the referenced device, fabricated Q-DSSCs displayed much better long-term stability.

CONCLUSIONS

In situ thermal polymerization of a model ionic liquid monomer and ionic liquids mixtures to form gel electrolytes after adding a series of I_2 have been prepared, investigated, and employed to fabricate Q-DSSCs without any volatile solvent. The devices based on the gel electrolytes showed a maximum efficiency of 5.01% under simulated full solar spectrum illumination. The excellent long-term stability indicated that the Q-DSSCs based on the gel electrolytes without any volatile solvent *in situ* thermal polymerization could overcome the leakage problem and high-temperature instability of liquid-state electrolytes. These results demonstrate a feasible approach to assemble high-performance Q-DSSCs in future practical applications.

ACKNOWLEDGMENTS

This work was supported by Jiangsu Fund for Distinguished Young Scientist (BK20140010), the Natural Science Foundation of Jiangsu Province (No. BK20140311), University Science Research Project of Jiangsu Province (No. 13KJB150033), the Open Foundation of

Jiangsu Key Laboratory of Thin Films, and the Project Funded by the PAPD of Jiangsu Higher Education Institutions.

REFERENCES

1. Grätzel, M. *Nature* **2001**, *414*, 338.
2. Hagfeldt, A.; Boschloo, G.; Sun, L.; Kloo, L.; Pettersson, H. *Chem. Rev.* **2010**, *110*, 6595.
3. Yella, A.; Lee, H. W.; Tsao, H. N.; Yi, C.; Chandiran, A. K.; Nazeeruddin, M. K.; Diau, E. W. G.; Yeh, C. Y.; Zakeeruddin, S. M.; Gratzel, M. *Science* **2011**, *334*, 629.
4. Mathew, S.; Yella, A.; Gao, P.; Humphry-Baker, R.; Curchod, B. F. E.; Ashari-Astani, N.; Tavernelli, I.; Rothlisberger, U.; Nazeeruddin, M. K.; Grätzel, M. *Nat. Chem.* **2014**, *6*, 242.
5. Wu, J. H.; Lan, Z.; Lin, J. M.; Huang, M. L.; Huang, Y. F.; Fan, L. Q.; Guo, G. G. *Chem. Rev.* **2015**, *115*, 2136.
6. Sathiya, A. R.; Subramania, A.; Jung, Y. S.; Kim, J. *Langmuir* **2008**, *24*, 9816.
7. Han, H.; Liu, W.; Zhang, J.; Zhao, X. *Adv. Funct. Mater.* **2005**, *15*, 1940.
8. Freitas, J. N. D.; Nogueira, A. F.; De Paoli, M-A. D. *J Mater. Chem.* **2009**, *19*, 5279.
9. Wu, J.; Hao, S.; Lan, Z.; Lin, J.; Huang, M.; Fang, L.; Yin, S.; Sato, T. *Adv. Funct. Mater.* **2007**, *17*, 2645.
10. Wu, J.; Hao, S.; Lan, Z.; Lin, J.; Huang, M.; Huang, Y.; Li, P.; Sato, T. *J. Am. Chem. Soc.* **2008**, *130*, 11568.
11. Gorlov, M.; Kloo, L. *Dalton. Trans.* **2008**, 2655.
12. Sun, Z.; Liang, M.; Chen, J. *Acc. Chem. Res.* **2015**, *48*, 1541.
13. Yao, Z. Y.; Zhang, M.; Wu, H.; Yang, L.; Li, R. Z.; Wang, P. *J. Am. Chem. Soc.* **2015**, *137*, 3799.
14. Lin, B.; Shang, H.; Chu, F.; Ren, Y.; Yuan, N.; Jia, B.; Zhang, S.; Yu, X.; Wei, Y.; Ding, J. *Electrochim. Acta* **2014**, *134*, 209.
15. Lin, B.; Feng, T.; Chu, F.; Zhang, S.; Yuan, N.; Qiao, G.; Ding, J. *RSC Adv.* **2015**, *5*, 57216.
16. Theerthagiri, J.; Senthil, R. A.; Ali@Buraidah, M. H.; Madhavan, J.; Arof, A. K. M. *J. Appl. Polym. Sci.* **2015**, DOI: 10.1002/APP.42489.
17. Welton, T. *Chem. Rev.* **1999**, *99*, 2071.
18. Rogers, R. D.; Seddon, K. R.; Voljov, S. In Green Industrial Applications of Ionic Liquids; NATO Science Series: Kluwer: Boston, **2002**.
19. Illeperuma, O. A.; Dissanayake, M. A. K. L.; Somasundaram, S.; Bandara, L. R. A. K. *Sol. Energy Mater. Sol. Cells* **2004**, *84*, 117.
20. Biancardo, M.; West, K.; Krebs, F. C. *Sol. Energy Mater. Sol. Cells* **2006**, *90*, 2575.
21. Kubo, W.; Kitamura, T.; Hanabusa, K.; Wada, Y.; Yanagida, S. *Chem. Commun.* **2002**, 374.
22. Wang, M.; Pan, X.; Fang, X.; Guo, L.; Liu, W.; Zhang, C.; Huang, Y.; Hu, L.; Dai, S. Y. *Adv. Mater.* **2010**, *22*, 5526.
23. Suzuki, K.; Yamaguchi, M.; Hotta, S.; Tanabe, N.; Yanagida, S. *J. Photochem. Photobiol. A Chem.* **2004**, *164*, 81.
24. Matsumoto, M.; Miyazaki, H.; Matsuhiro, K.; Kumashiro, Y.; Takaoka, Y. *Solid State Ionics* **1996**, *89*, 263.
25. Kubo, W.; Makimoto, Y.; Kitamura, T.; Wada, Y.; Yanagida, S. *Chem. Lett.* **2002**, 948.
26. Xiang, W.; Zhou, S.; Yin, X.; Fang, S. *Polym. Adv. Technol.* **2009**, *20*, 519.
27. Winther-Jensen, O.; Armel, V.; Forsyth, M.; Macfarlane, D. R. *Macromol. Rapid. Commun.* **2010**, *31*, 479.
28. Wang, L.; Fang, S. B.; Lin, Y.; Zhou, X. W.; Li, M. Y. *Chem. Commun.* **2005**, 5687.
29. Bonhte, P.; Dias, A. P.; Papageorgiou, N.; Kalyanasundaram, K.; Grätzel, M. *Inorg. Chem.* **1996**, *35*, 1168.
30. Nazeeruddin, M. K.; Kay, A.; Rodicio, I.; Humphry-Baker, R.; Muller, E.; Liska, P.; Vlachopoulos, N.; Grätzel, M. *J. Am. Chem. Soc.* **1993**, *115*, 6382.
31. Orel, B.; SurcaVuk, A.; Jese, R.; Lianos, P.; Stathatos, E.; Judeinstein, P. *Solid State Ionics* **2003**, *165*, 235.
32. Yu, Z.; Gorlov, M.; Nissfolk, J.; Boschloo, G.; Kloo, L. *J. Phys. Chem. C* **2010**, *114*, 10612.
33. Kang, M. S.; Kim, J. H.; Won, J.; Kang, Y. S. *J. Phys. Chem. C* **2004**, *111*, 5222.
34. Benedetti, J. E.; De Paoli, M. A.; Nogueira, A. F. *Chem. Commun.* **2008**, 1121.
35. Kubo, W.; Kambe, S.; Nakade, S.; Kitamura, T.; Hanabusa, K.; Wada, Y.; Yanagida, S. 2003, *J. Phys. Chem. B* **2003**, *107*, 4374.
36. Wang, G.; Wang, L.; Zhuo, S.; Fang, S.; Lin, Y. *Chem. Commun.* **2010**, *47*, 2700.
37. Zhao, J.; Yan, F.; Chen, Z.; Diao, H.; Chu, F.; Yu, S.; Lu, J. *J. Polym. Sci. Part A Polym. Chem.* **2009**, *47*, 746.
38. Marcilla, R.; Sanchez-Paniagua, M.; Lopez-Ruiz, B.; Cabarcos, E.; Ochoteco, E.; Grande, H.; Mecerreyes, D. *J. Polym. Sci. Part A Polym. Chem.* **2006**, *44*, 3958.
39. Cong, S.; Yi, Q. H.; Wang, Y.; Zhao, J.; Sun, Y. H.; Zou, G. F. *J. Power Source* **2015**, *280*, 90.
40. Zhao, J.; Yan, F.; Qiu, L.; Zhang, Y.; Chen, C.; Sun, B. *Chem. Commun.* **2011**, *47*, 11516.